J. Austral. Math. Soc. Ser. B 41(2000), 338–357

AN ANALYSIS OF TWO AND THREE DIMENSIONAL UNSTEADY WITHDRAWAL FLOWS, USING SHALLOW WATER THEORY

A. J. KOERBER[1] and L. K. FORBES[1]

(Received 30 August 1996; revised 24 December 1997)

Abstract

This paper examines the predictions of shallow water theory for steady and unsteady withdrawal flows through an extended sink from fluid of finite depth. Two-dimensional plane flows and three-dimensional axi-symmetric flow through a circular drain are examined. Shallow water theory indicates the presence of limiting configurations, where the surface of the fluid collapses directly into the sink. In addition, this theory suggests that some previously computed steady solutions may be unstable.

1. Introduction

There has been much interest recently in the field of withdrawal flows with a free surface, with much attention given to two-dimensional withdrawal flows due to a line sink, although three-dimensional flows into a point sink are also receiving increased attention. Tuck and Vanden Broeck [12] did pioneering work on the two-dimensional problem, studying the flow due to a sink in a fluid of infinite depth. They found a cusped free surface for a unique Froude number and also mentioned the existence of solutions with a stagnation point on the free surface, rather than a cusp. Mekias and Vanden-Broeck [9] furthered this work by finding steady supercritical stagnation solutions for a point sink in a finite-depth fluid. In a later paper (Mekias and Vanden-Broeck [10]) they found that subcritical flows exist but exhibit waves. However, Hocking and Forbes [5] found stagnation solutions without the existence of waves. This issue is not yet resolved. Hocking [4] looked at withdrawal into a vertical slot and found cusp-like solutions in which the free surface was drawn right down into the slot; these were only possible for supercritical flow.

In three dimensions, withdrawal flow due to a point sink has been studied by Forbes and Hocking [1] for fluid of infinite depth, and Forbes, Hocking and Chandler [3] for

[1]Department of Mathematics, University of Queensland, Brisbane, QLD 4072, Australia.

fluid of a finite depth. They found stagnation solutions, similar to those in two dimensions, which exist up to a limiting value of the Froude number. Flow due to an extended circular sink was investigated by Forbes and Hocking [2]. They considered the case where the free surface has dropped into the sink in a fluid rotating due to a vortex as well as the non-rotating stagnation flow case. Ivey and Blake [6] and Zhou and Graebel [13] have also studied axi-symmetric withdrawal flows, with the former putting some emphasis on experimental work.

Thus, in both two-dimensional and three-dimensional withdrawal flows, it has been found that limiting values of the Froude number (fluid withdrawal rate) apparently exist, beyond which there may not be steady solutions. A physical explanation for this observation is lacking in most cases, however. This is largely due to the fact that the mathematical equations describing these flows are complicated non-linear partial differential equations, for which the only possible solutions are numerical. A simpler theory is needed, to provide at least a qualitative explanation of these phenomena, since this information is not easily available from difficult numerical solution codes.

The purpose of this paper is to suggest that a plausible explanation for much of this behaviour in withdrawal flows is provided by classical shallow water theory, as outlined in texts such as Stoker [11], for example. In this simple hydraulic theory, vertical velocity components are essentially ignored. It appears that the useful insights provided by this simplified approach have been largely overlooked, in the context of withdrawal flows.

Here we investigate two- and three-dimensional extended sink problems using shallow water theory. This approximation lends itself to a simple analysis and gives closed form solutions. It is found to confirm many of the known features of two- and three-dimensional stagnation flows, as well as providing a partial explanation for the existence of the limiting Froude numbers for such flows and suggests what is likely to happen to the flow when the Froude number is increased beyond these limits.

2. Steady 2D withdrawal

The problem we consider is the irrotational flow of an inviscid, incompressible fluid through a slot-like drain of width $2L$, with a free surface above the drain. We impose a constant exit speed (and hence constant volume flux $2Q$) and assume the fluid is of infinite lateral extent. The x-axis is chosen to lie along the flat bottom of the fluid and the y-axis is chosen to go through the centre of the drain.

In two dimensions the fluid velocity vector is $\mathbf{q} = u\mathbf{i} + v\mathbf{j}$ where the horizontal and vertical components of velocity u and v are functions of the independent variables x and y. The position of the free surface is given by $y = \eta(x)$, the pressure and the gravitational acceleration are denoted by P and g respectively. We introduce

https://doi.org/10.1017/S0334270000011280 Published online by Cambridge University Press

dimensionless variables

$$\hat{x} = \frac{x}{H}, \quad \hat{y} = \frac{y}{H}, \quad \hat{\eta} = \frac{\eta}{H},$$
$$\hat{u} = \frac{u}{\sqrt{gH}}, \quad \hat{v} = \frac{v}{\sqrt{gH}}, \quad \hat{P} = \frac{P}{\rho g H},$$

in which the upstream depth H of the fluid is taken as the characteristic length scale, and $\sqrt{gH}$ is the unit of speed. This non-dimensionalisation introduces a parameter $\hat{L} = L/H$ which is half the drain width scaled by the upstream depth. The hats above non-dimensional quantities shall be dropped through the rest of the discussion. The geometry of the problem is shown in Figure 1.

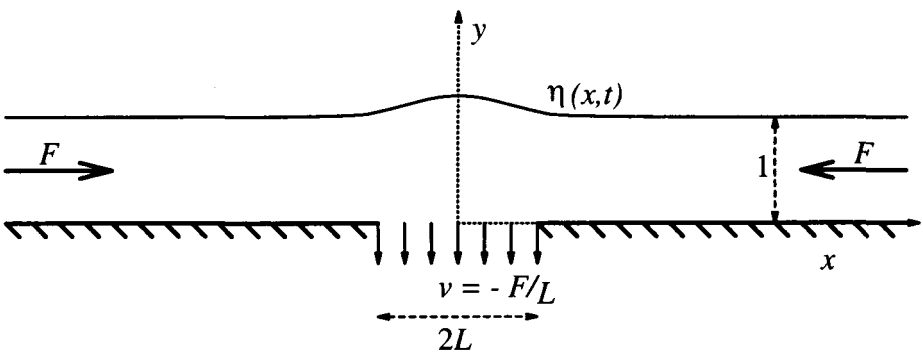

FIGURE 1. A sketch in dimensionless coordinates showing the extended sink withdrawal problem. The outflow speed is $-F/L$.

We approximate the flow using the well-known equations of shallow water theory, which may be found in many classical texts, such as the book by Stoker [11]. These are an approximation to the full Eulerian equations of motion under the assumption that the vertical component of velocity is small, or equivalently, that the pressure within the fluid remains hydrostatic. Conservation of mass is expressed by the equation

$$\frac{d(u\eta)}{dx} = \begin{cases} 0, & |x| > L, \\ -\dfrac{F}{L}, & |x| < L, \end{cases} \tag{1}$$

where $F = Q/\sqrt{gH^3}$ is the Froude number and Q is the volume flux through the drain. The conservation of momentum in the x-direction becomes, in this approximation,

$$u\frac{du}{dx} + \frac{d\eta}{dx} = 0. \tag{2}$$

https://doi.org/10.1017/S0334270000011280 Published online by Cambridge University Press

Due to the symmetry of the flow about the y-axis only the flow for $x > 0$ need be considered, as the flow for $x < 0$ can be obtained by reflection. Equation (1) may be integrated at once to yield

$$u\eta = \begin{cases} -F, & x > L, \\ -\dfrac{F}{L}x, & 0 \le x < L, \end{cases} \tag{3}$$

where the conditions $u \to -F$, $\eta \to 1$ as $x \to \infty$ have been applied. Similarly, (2) can be integrated easily to give

$$\frac{1}{2}u^2 + \eta = \frac{1}{2}F^2 + 1, \tag{4}$$

where again, boundary conditions at infinity have been applied.

Outside the region of the drain, $x > L$, (3) and (4) show that the surface is simply flat. Thus

$$u = -F \quad \text{and} \quad \eta = 1 \quad \text{for} \quad x > L. \tag{5}$$

Above the drain, in the region $0 \le x < L$, the conditions (3) and (4) may be combined to yield the cubic equation

$$\eta^3 - \left(1 + \frac{F^2}{2}\right)\eta^2 + \frac{F^2}{2L^2}x^2 = 0, \qquad 0 \le x < L \tag{6}$$

for the surface elevation $\eta(x)$. Note that, at $x = 0$, this equation predicts that $\eta(0) = 1 + F^2/2$, which is in agreement with the exact solution for the maximum height obtained from the Bernoulli equation in the full non-linear theory. It can also be seen in (6) that the dependence of the surface elevation varies only with the square of the Froude number F. Therefore, these equations predict the surface elevation will be the same for an extended sink or an extended *source* of the same strength. For practical numerical evaluation purposes, (6) can be re-arranged to give x explicitly in terms of η,

$$x = \pm\frac{\sqrt{2}L}{F}\eta\sqrt{\left(1 + \frac{F^2}{2}\right) - \eta}. \tag{7}$$

Figure 2 shows three surfaces for differing Froude numbers and drain width $2L = 2$. The solid line represents a solution for $F = 0.5$ and the two larger amplitude disturbances correspond to $F = 1$ and $F = 1.5$. The case $F = 0.5$ is possibly a reasonable approximation to the full non-linear solution, under appropriate circumstances. However, the supercritical solution, obtained with $F = 1.5$, seems unphysical since the

https://doi.org/10.1017/S0334270000011280 Published online by Cambridge University Press

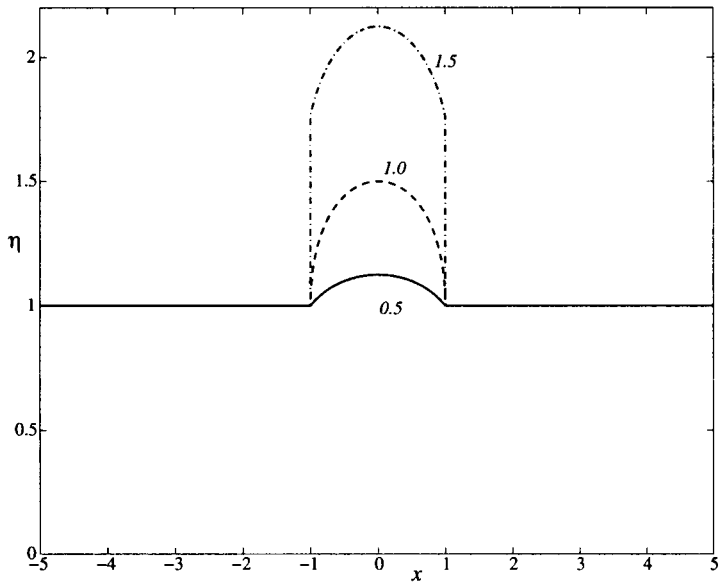

FIGURE 2. Three typical two-dimensional steady stagnation point solution surface elevation profiles for $L = 1$ and $F = 0.5$ (solid line), 1.0 (dashed line) and 1.5 (dash-dot line).

surface becomes vertical at the drain edges, $x = \pm 1$. Nevertheless, solutions of this type were found in the fully non-linear problem by Mekias and Vanden-Broeck [9], although in their exact formulation, the surface rose smoothly to its stagnation point. It is reasonable to expect this solution for $F = 1.5$ in Figure 2 to be unstable.

We now seek to determine for what value of the Froude number the surface elevation first becomes vertical. From (6) we have

$$\frac{d\eta}{dx} = \frac{(F^2/L^2)x}{(1 + F^2/2)2\eta - 3\eta^2}.$$

This derivative is indeterminate at $\eta = 0$ and becomes infinite at $\eta = 2(1 + F^2/2)/3$, where $x = \pm(L/F)[2(1 + F^2/2)/3]^{3/2}$, by (7). Hence the surface slope is infinite at $\eta = 1$ (where it joins the undisturbed surface) for $F = 1$. Therefore, all supercritical solutions ($F > 1$) will possess vertical portions, similar to the situation with $F = 1.5$ shown in Figure 2, if the surface rises to a stagnation point.

Conversely, (6) has solutions for $\eta < 1$ as shown in Figure 3, for the same three Froude numbers as in Figure 2. These all have the surface dipping so that it just touches the extended sink at the origin. In the case that the surface touches the sink, it must do so at the origin, due to the symmetry of the problem and to conserve mass, since the outflow velocity is $-F/L$.

The $F = 0.5$ solution in Figure 3 is now expected to be unphysical since it possesses

https://doi.org/10.1017/S0334270000011280 Published online by Cambridge University Press

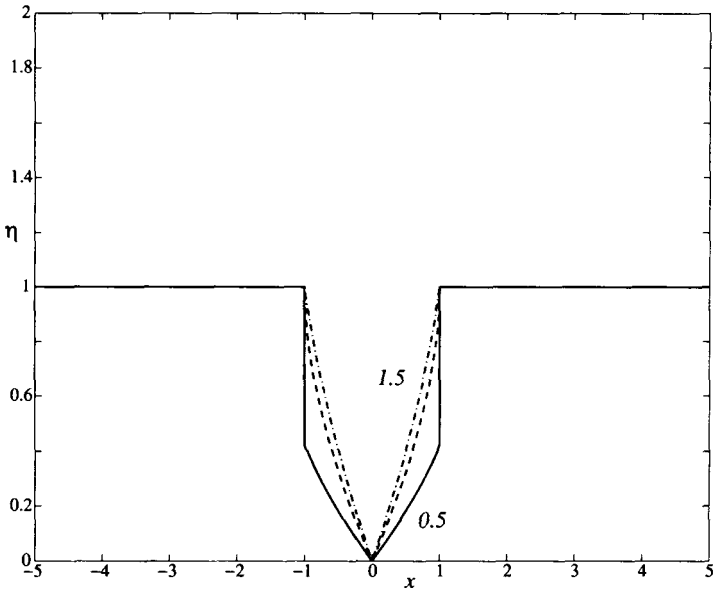

FIGURE 3. The surface elevation profiles for three 'drawn-down' steady solutions for $L = 1$ and $F = 0.5$ (solid line), 1.0 (dashed line) and 1.5 (dash-dot line).

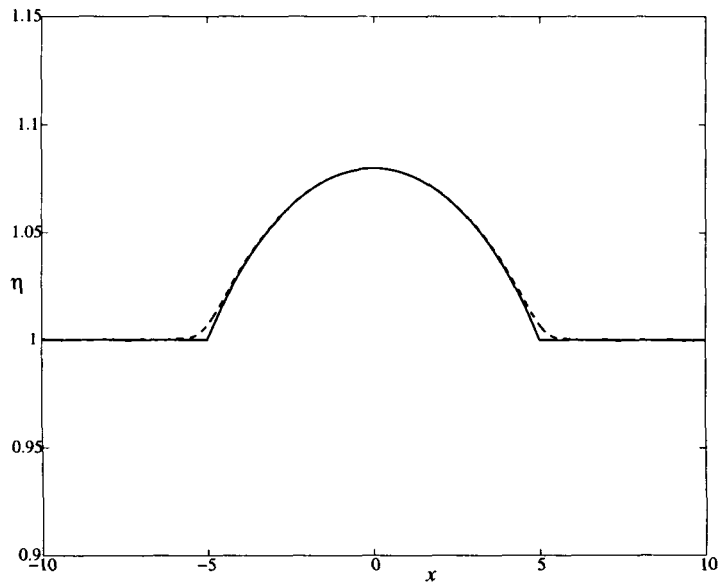

FIGURE 4. A comparison between the shallow water approximation (solid line) and the full non-linear solution (dashed line) for a stagnation point flow with $F = 0.4$ and $L = 5$.

https://doi.org/10.1017/S0334270000011280 Published online by Cambridge University Press

vertical segments, but the solutions for $F \geq 1$ could well be valid. We suggest that this is indeed what shallow water theory is predicting, namely that the stagnation solutions as in Figure 2 exist only up to $F = 1$ and then the surface is drawn down into the sink for $F > 1$, as in Figure 3. Similar drawn-down solutions to the full non-linear equations have been found by Hocking [4] and he likewise determined that they only exist for Froude numbers greater than 1. The limiting drawn-down surface shape as $F \to \infty$ can easily be observed from (6) to be $\eta \to \pm x/L$. This is already closely approximated by the $F = 1.5$ solution in Figure 3.

Notice that Figures 2 and 3 show two different solution types for the same problem, at the same given Froude numbers. From the above discussion, it appears that the solution type in Figure 2 is stable for $F < 1$ and the solution type in Figure 3 is stable for $F > 1$.

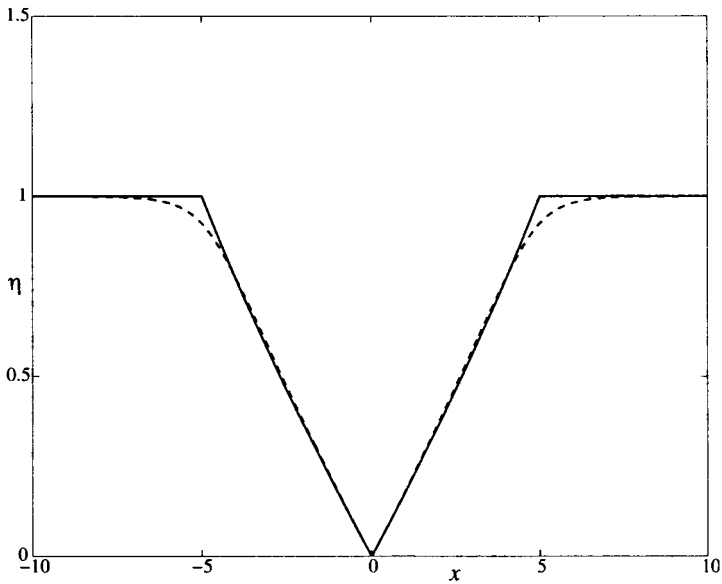

FIGURE 5. A comparison between the shallow water (solid line) and non-linear (dashed line) 'drawn-down' solutions for $F = 2.5$ and $L = 5$.

Figure 4 shows the comparison between the shallow water stagnation solution for a Froude number of $F = 0.4$ and drain width $2L = 10$, with the corresponding full non-linear stagnation solution. Similarly, Figure 5 shows the shallow water drawn-down solution together with the full non-linear drawn-down solution for $F = 2.5$ and a drain width of $2L = 10$. These figures show very good agreement between the shallow water solutions and the non-linear solutions. This agreement improves as the drain width increases, as a wider drain width (and hence smaller vertical exit speed) is more consistent with the shallow water approximation. The non-linear solutions

https://doi.org/10.1017/S0334270000011280 Published online by Cambridge University Press

presented are obtained by an integral equation technique, the details of which shall appear in a future publication.

3. Numerical solution for the 2D unsteady problem

The unsteady shallow water equations for two-dimensional flow written in conservation form are

$$\frac{\partial \phi}{\partial t} + \frac{\partial}{\partial x}\left(\frac{\phi^2}{\eta} + \frac{1}{2}\eta^2\right) = \begin{cases} 0, & |x| > L, \\ -(F/L)\,\phi/\eta, & |x| < L, \end{cases} \tag{8}$$

$$\frac{\partial \eta}{\partial t} + \frac{\partial(\phi)}{\partial x} = \begin{cases} 0, & |x| > L, \\ -F/L, & |x| < L. \end{cases} \tag{9}$$

where $\phi = u\eta$ is equivalent to momentum and η is equivalent to mass.

Equations (8) and (9) are solved using MacCormack's method (see LeVeque [7] or MacCormack [8]) for a system of hyperbolic PDE's in conservation form. It is modified to include the source term on the right-hand side of (9). This was found to be by far the best method out of the several trialed, especially for the three-dimensional axi-symmetric case (see Section 6).

The spatial domain from $x = -10$ to $x = 10$ is discretised evenly onto a grid of 3200 divisions. The time step size is chosen to be $\Delta t = 0.004\Delta x$. The numerical solution was not found to be significantly affected by decreasing the time step size.

The numerical scheme is

$$\begin{aligned} \bar{\mathbf{U}}_j^{n+1} &= \mathbf{U}_j^n - \frac{\Delta t}{\Delta x}\left[\mathbf{F}_{j+1}^n - \mathbf{F}_j^n\right] + \Delta t\left[\mathbf{B}_j^n\right], \\ \mathbf{U}_j^{n+1} &= \frac{1}{2}\left[\mathbf{U}_j^n + \bar{\mathbf{U}}_j^{n+1}\right] - \frac{\Delta t}{2\Delta x}\left[\bar{\mathbf{F}}_j^{n+1} - \bar{\mathbf{F}}_{j-1}^{n+1}\right] + \frac{\Delta t}{2}\left[\bar{\mathbf{B}}_j^{n+1}\right], \end{aligned} \tag{10}$$

where

$$\mathbf{U}_j^n = \begin{bmatrix} \phi_j^n \\ \eta_j^n \end{bmatrix}, \quad \mathbf{F}_j^n = \begin{bmatrix} (\phi_j^n)^2/\eta_j^n + (\eta_j^n)^2/2 \\ \phi_j^n \end{bmatrix} \quad \text{and} \quad \mathbf{B}_j^n = \begin{cases} \begin{bmatrix} 0 \\ 0 \end{bmatrix}, & |x| > L \\ \begin{bmatrix} -(F/L)\,\phi_j^n/\eta_j^n \\ -F/L \end{bmatrix}, & |x| < L. \end{cases}$$

This is subject to the boundary conditions

$$\frac{\partial \eta}{\partial t} = \frac{\partial \phi}{\partial t} = 0 \quad \text{at} \quad x = \pm 10.$$

https://doi.org/10.1017/S0334270000011280 Published online by Cambridge University Press

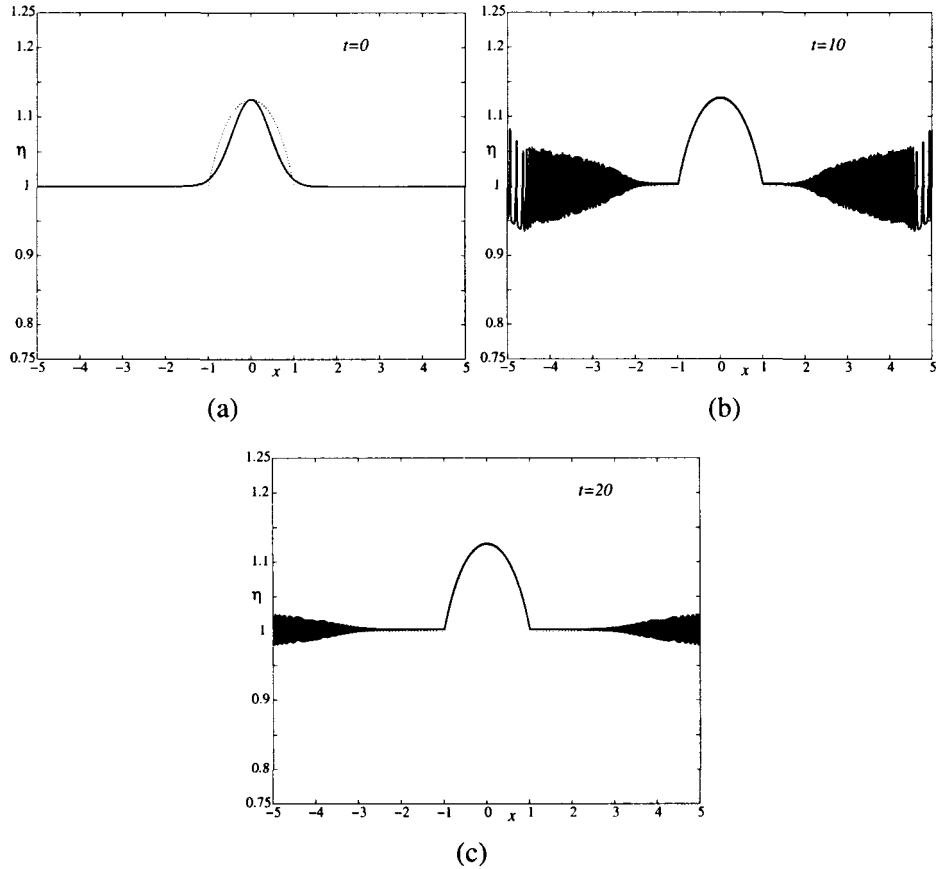

FIGURE 6. The evolution of an initial guess to the free surface stagnation solution, for $L = 1$ and $F = 0.5$, at times (a) $t = 0$ (b) $t = 10$ and (c) $t = 20$. The solid line is the numerical solution and the dotted line is the steady solution.

An approximation to the initial surface profile for a Froude number of $F = 0.5$ and drain width of $2L = 2$ is generated by the function $\eta_i = 1 + Fe^{-5/2x_i^2}$. The corresponding velocities u_i are obtained from (4) for steady flow. Figures 6(a)–(c) show the evolution of this surface for $t = 0$, $t = 10$ and $t = 20$. In Figure 6(a), the initial condition, given by the exponential function discussed above, is shown with a solid line, while the dotted line corresponds to the steady solution (5) and (6). By $t = 10$ (Figure 6(b)) it can be seen that in the interval $|x| < 1$ the surface has already settled down to the steady-state solution, with the large numerical residue from the startup moving away in the negative and positive x directions. These residues are numerical in origin and have no physical significance. At $t = 20$ (Figure 6(c)) we see that the numerical residue has moved further away from the steady solution area. This behaviour is also observed for other Froude numbers less than one. We note

https://doi.org/10.1017/S0334270000011280 Published online by Cambridge University Press

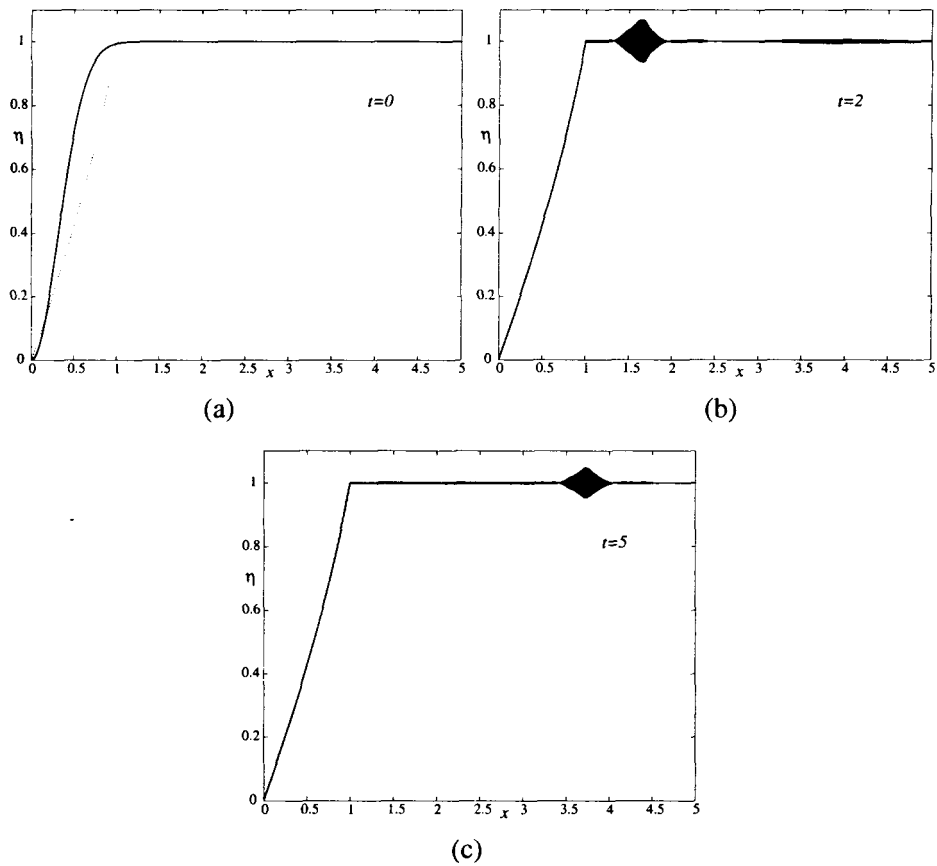

FIGURE 7. The behavior of the 'drawn-down' solution for $L = 1$ and $F = 1.7$ with the $x = 0$ point fixed at $\eta = 0$, starting from an initial guess, at times (a) $t = 0$ (b) $t = 2$ and (c) $t = 5$. The solid line is the numerical solution and the dotted line is the steady solution.

however, that the numerical solution is not converging exactly to the steady solution, since for $|x| > 1$ the solution is generating an elevation just above $y = 1$. This is due to the large difference between the initial guess and actual steady-state solution, and the large numerical oscillations thereby thrown off, which are in effect creating a higher surface elevation boundary condition in the far-field. We hence conclude that all stagnation point solutions are stable for $F < 1$. As expected from this, the solutions where the free surface drops to touch the sink at $x = 0$ are found to be unstable for $F < 1$.

For $F > 1$ the numerical solution is inconclusive for both stagnation point solutions and the drawn-down solutions, although the instability in the drawn-down case is associated with the $x = 0$ point. Specifically, for steady flow, y must equal zero at $x = 0$. But when the numerical noise takes the free surface just below $y = 0$ (which

https://doi.org/10.1017/S0334270000011280 Published online by Cambridge University Press

is an unphysical situation), the numerical method rapidly becomes unstable and fails, as is to be expected.

We now fix the solution at $x = 0$ by imposing the steady solution at that point. In the case of the solution that just touches the sink at $x = 0$ we fix $\eta = 0$ and $u = -\sqrt{2(1 + 1/2F^2)}$ from (4). To test the stability of the drawn-down solution with the $x = 0$ point fixed, an initial approximation to the surface elevation is generated by $\eta_i = 1 - e^{-5x_i}$ for $x_i > 0$ and an initial guess to the horizontal velocities u_i is again obtained from (4) where the Froude number is chosen to be $F = 1.7$ and the drain width is again chosen to be $2L = 2$. Figures 7(a)–(c) show the surface for this Froude number at times $t = 0$, 2 and 5. Again, the solid line in Figure 7(a) represents the initial condition, and the dotted line is the final steady solution obtained from (5) and (6). By time $t = 2$ (Figure 7(b)) the surface for $0 < x < 1$ has converged to the steady solution and shed off a wave-packet of noise which continues to move away from $x = 0$ as can be seen at $t = 5$ in Figure 7(c). Tiny grid scale oscillations exist, starting at $x = 1$ and extending in the positive x direction. These are caused by the discontinuity in the bottom boundary condition due to the sink. A linear velocity profile for the sink was trialed, so that the boundary condition was continuous at $|x| = 1$. This did indeed remove the tiny grid scale noise, but in all respects remained qualitatively the same as for the discontinuous (and simpler) case presented.

When the solution at $x = 0$ is fixed at the steady stagnation height, that is $\eta = 1 + 1/2F^2$ ($u = 0$), for $F > 1$, numerical noise from the jump discontinuity in the steady stagnation solution for $F > 1$ causes the numerical scheme to break down. Therefore, results for the stagnation solution in the supercritical regime remain inconclusive. However, due to the evidence described above, we suspect that the drawn-down surface solution is indeed the stable solution for $F > 1$ and that the stagnation point solutions become unstable.

4. Withdrawal from 3D sink

Here we consider the unsteady flow through a circular drain of radius A, with constant withdrawal rate Q. We consider only axi-symmetric flow and assume the fluid is of infinite radial extent. Three-dimensional cylindrical polar co-ordinates are chosen such that the axis of the radial co-ordinate r lies along the level bottom of the fluid and the vertical axis z is in the centre of the circular drain. In these co-ordinates, the axi-symmetric fluid velocity vector is $\mathbf{q} = u\mathbf{e}_r + v\mathbf{e}_\theta + w\mathbf{k}$, where the radial velocity component u, the azimuthal velocity component v and the vertical velocity component w are all functions of the cylindrical polar co-ordinates r and z and of time t. The position of the free surface is given by $z = \zeta(r, t)$, the pressure in the fluid is denoted by $P(r, z, t)$ and gravitational acceleration is denoted by g.

https://doi.org/10.1017/S0334270000011280 Published online by Cambridge University Press

Euler's equations expressing the conservation of momentum in cylindrical polar co-ordinates under the assumption of axi-symmetry are

$$\begin{aligned}
&\frac{\partial u}{\partial t} + u\frac{\partial u}{\partial r} + w\frac{\partial u}{\partial z} - \frac{v^2}{r} = -\frac{1}{\rho}\frac{\partial P}{\partial r},\\
&\frac{\partial v}{\partial t} + u\frac{\partial v}{\partial r} + w\frac{\partial v}{\partial z} + \frac{uv}{r} = 0,\\
&\frac{\partial w}{\partial t} + u\frac{\partial w}{\partial r} + w\frac{\partial w}{\partial z} = -g - \frac{1}{\rho}\frac{\partial P}{\partial z}.
\end{aligned} \tag{11}$$

The continuity equation, which represents the conservation of mass, is

$$\frac{1}{r}\frac{\partial (ru)}{\partial r} + \frac{\partial w}{\partial z} = 0. \tag{12}$$

We again introduce non-dimensional variables

$$\hat{r} = \frac{r}{H}, \quad \hat{z} = \frac{z}{H}, \quad \hat{\zeta} = \frac{\zeta}{H},$$
$$\hat{u} = \frac{u}{\sqrt{gH}}, \quad \hat{v} = \frac{v}{\sqrt{gH}}, \quad \hat{w} = \frac{z}{\sqrt{gH}}, \quad \hat{P} = \frac{P}{\rho g H}, \quad \hat{t} = t\sqrt{\frac{g}{H}}.$$

Here the undisturbed depth of the fluid H is taken as the characteristic length scale and $\sqrt{gH}$ the characteristic speed scale. This introduces a parameter $\alpha = A/H$, which is the drain radius made dimensionless with respect to the upstream fluid depth. Note that α plays precisely the same role as the constant width L in the two-dimensional withdrawal case in (1).

Now we make the shallow water approximation that the vertical velocity component w is negligible in the momentum equations while $\partial w/\partial z$ remains order 1 in the continuity equation. Also assuming that no rotation occurs, that is $v(r, t) \equiv 0$, (11) reduces to

$$\frac{\partial u}{\partial t} + u\frac{\partial u}{\partial r} = -\frac{\partial P}{\partial r}, \tag{13}$$

$$-1 - \frac{\partial P}{\partial z} = 0, \tag{14}$$

in dimensionless form (where the hats above non-dimensional quantities have again been dropped, as in Section 2).

These equations are subject to the following boundary conditions along the bottom

$$\begin{aligned}
&w = 0 \quad \text{on} \quad r > \alpha,\\
&w = -\frac{F}{\pi\alpha^2} \quad \text{on} \quad 0 \le r < \alpha,
\end{aligned} \tag{15}$$

https://doi.org/10.1017/S0334270000011280 Published online by Cambridge University Press

where $F = Q/\sqrt{gH^5}$ is the Froude number for three-dimensional flows. On the free surface of the fluid we have the dynamic condition

$$P = 0 \quad \text{on} \quad z = \zeta(r) \tag{16}$$

and the kinematic condition

$$\frac{\partial \zeta}{\partial t} = w - u\frac{\partial \zeta}{\partial r} \quad \text{on} \quad z = \zeta(r). \tag{17}$$

Equation (14) is integrated and the surface pressure condition (16) is used to give the hydrostatic equation $P(r, z, t) = \zeta(r, t) - z$. The continuity equation (12) is integrated from the fixed bottom $z = 0$ to the free surface $z = \zeta$ and the boundary conditions (15) and (17) are applied to yield

$$\frac{1}{r}\frac{\partial (ru)}{\partial r}\zeta + u\frac{\partial \zeta}{\partial r} + \frac{\partial \zeta}{\partial t} = \begin{cases} 0 & r > \alpha, \\ -F/(\pi\alpha^2) & 0 \le r < \alpha. \end{cases} \tag{18}$$

It is convenient to write (13) and (18) in conservation form. This form will be specifically exploited in Section 6. The system of conservation equations is

$$\frac{\partial u}{\partial t} + \frac{\partial}{\partial r}\left(\frac{1}{2}u^2 + \frac{\chi}{r}\right) = 0, \tag{21}$$

$$\frac{\partial \chi}{\partial t} + \frac{\partial}{\partial r}(u\chi) = \begin{cases} 0 & r > \alpha, \\ -rF/(\pi\alpha^2) & 0 \le r < \alpha, \end{cases} \tag{20}$$

where $\chi = r\zeta$.

5. Steady 3D flow

In the steady case, the radial velocity u and the surface elevation ζ do not depend on time, so are only functions of the radial co-ordinate r. Since the time derivatives in (19) and (20) are zero, the equations may be immediately integrated with respect to r to give

$$u^2/2 + \zeta = 1, \tag{21}$$

$$ur\zeta = \begin{cases} -F/(2\pi) & r > \alpha, \\ -r^2F/(2\pi\alpha^2) & 0 \le r < \alpha, \end{cases} \tag{22}$$

in which the requirement that the flux $ur\zeta$ be continuous at $r = \alpha$ has been imposed and the far-field conditions have been applied. The far-field conditions are that $u \to 0$

https://doi.org/10.1017/S0334270000011280 Published online by Cambridge University Press

and $\zeta \to 1$ as $r \to \infty$ and that the volume flux $2\pi R u\zeta$, at a radius $R > \alpha$, balances the volume flux $-F$ through the drain.

Equations (21) and (22) can be combined to eliminate the velocity u and give an equation for the surface elevation ζ in terms of the radius. That is,

$$\zeta^2 - \zeta^3 = \begin{cases} F^2/(8\pi^2 r^2) & r > \alpha, \\ r^2 F^2/(8\pi^2 \alpha^4) & 0 \le r < \alpha. \end{cases} \tag{23}$$

As in the two-dimensional problem, here the shape of the surface elevation only depends on the square of the Froude number F, so that again, there is no difference to the surface elevation whether we have a sink or a *source*. This equation can be rearranged to give explicit equations for r in terms of ζ, making numerical calculation of the surface shape easier.

Figure 8 shows the graphs of these surfaces for three typical Froude numbers with the drain radius $\alpha = 1$. Here results are shown for $F = 1$, $F = 2$ and $F = 3$. In each case, shallow water theory (23) predicts a free surface stagnation point at the centre of the sink, where $(r, \zeta) = (0, 1)$, and a sharp dip at the edge of the drain, where $r = \alpha$.

Figure 9 shows the relationship between the shallow water solution and the full non-linear solution of Forbes and Hocking [2] for $F = 2$ and $\alpha = 5$. The exact solution possesses a smooth dip at about $r = \alpha$, rather than the sharp corner predicted by the shallow water theory. The same relationship between the shallow water and full non-linear solutions has been found to hold for all Froude numbers up to the limiting Froude number for the full non-linear case, for a given drain radius α. A radius of $\alpha = 5$ is chosen for the figure, as larger radii are more consistent with the shallow water approximation.

The derivative of the surface elevation ζ is found from (23) to be

$$\frac{d\zeta}{dr} = \begin{cases} -\dfrac{F^2}{4\pi^2 r^3 \zeta(2 - 3\zeta)} & r > \alpha, \\ \dfrac{rF^2}{4\pi^2 \alpha^4 \zeta(2 - 3\zeta)} & 0 \le r < \alpha, \end{cases}$$

and is discontinuous and changes sign at $r = \alpha$, and clearly tends to infinity as $\zeta \to 2/3$. At $\zeta = 2/3$, $u = -\sqrt{2/3}$ and substituting these together with $r = \alpha$ into (22) gives the critical Froude number at which this occurs,

$$F_{\text{crit}} = \pi\alpha(4/3)\sqrt{2/3} \approx 3.42013\alpha. \tag{24}$$

This would appear to be an overestimation of critical Froude number for the full non-linear case where $F_{\text{lim}} = 2.385$ for $\alpha = 1$, as calculated by Forbes and Hocking [2].

For Froude numbers less than the critical value (24), stagnation flows exist similar to those in Figure 8. At the critical Froude number, however, two solutions exist, the

https://doi.org/10.1017/S0334270000011280 Published online by Cambridge University Press

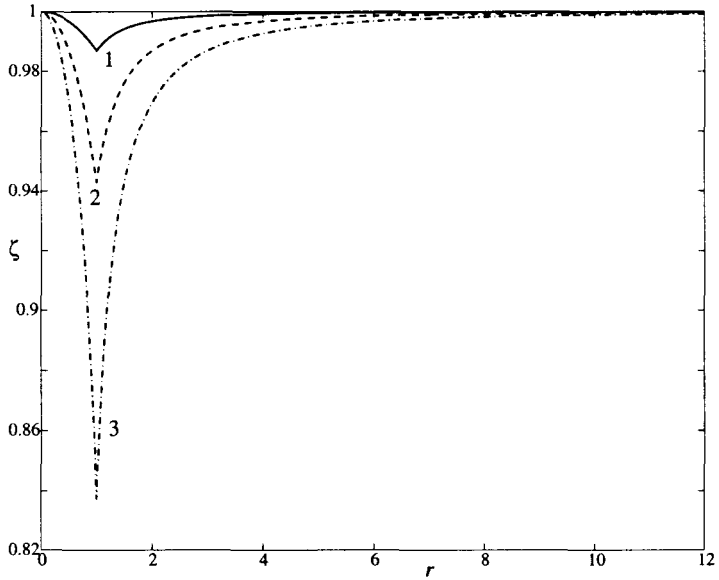

FIGURE 8. Three axi-symmetric stagnation point free surface profiles for $\alpha = 1$ and $F = 1.0$ (solid line), $F = 2.0$ (dashed line) and $F = 3.0$ (dash-dot line).

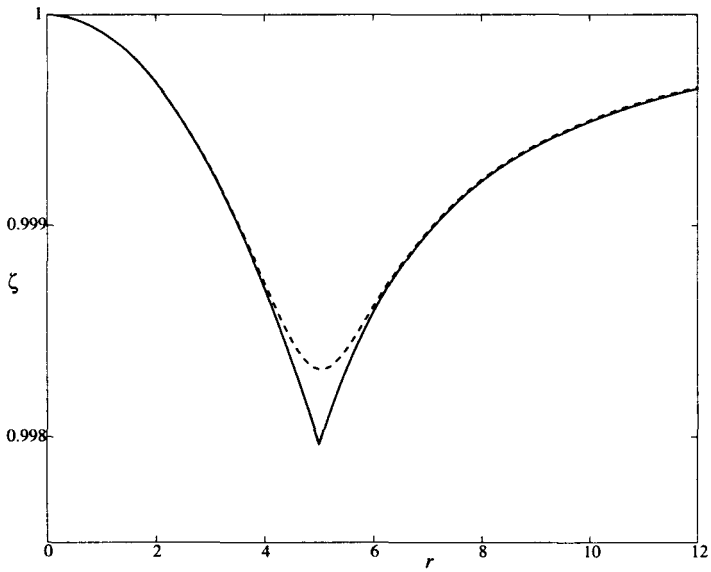

FIGURE 9. The relationship between the shallow water approximation (solid line) and full non-linear solution (Forbes and Hocking [2]) (dashed line) for $\alpha = 5$ and $F = 2$.

https://doi.org/10.1017/S0334270000011280 Published online by Cambridge University Press

typical stagnation flow in Figure 10(a) and another where the surface for $r < \alpha$ has dropped down to $\zeta = 0$ for $r = 0$, as shown in Figure 10(b). For Froude numbers greater than this critical value, no solutions are found to exist. It is noted that the drawn-down solution for $F = F_{\text{crit}}$ must have $u = -\sqrt{2}$ at $r = 0$ from (21) which violates the physical requirement that $u = 0$ at $r = 0$ by the nature of the co-ordinate system. However, since $\zeta = 0$ at $r = 0$ there is no actual horizontal volume flux occurring here.

Although the shallow water approximation is not valid for large values of the Froude number, the drawn-down solution at the critical Froude number tends to suggest that this is where a transition in the surface occurs, from a stagnation point solution to some type of flow in which the surface is drawn down into the sink.

6. Numerical solution for the 3D unsteady problem

In this section, the unsteady equations (19) and (20) are solved using MacCormack's method (see LeVeque [7]) as in Section 3. Equation (19) is used instead of the equation that would correctly express the momentum law in conservation form because of numerical difficulties associated with that more complicated momentum conservation equation, near $r = 0$. This will result in any shock speeds being incorrectly calculated, but since no shocks are present or expected, it will make no other significant difference. Furthermore, the two-dimensional problem was solved using two different conservation forms for the unsteady equations. One was the correct form presented in Section 3, (8) and (9), and the other a form analogous to (19). Even in this case, no qualitative difference was found between the two unsteady solutions.

The velocity and the surface elevation are discretised on an evenly spaced radial grid of 480 divisions with grid points $r_j = j\,\Delta r$ for $j = 0, \ldots, 480$. The radial domain is truncated at $r = 12$. In all numerical runs the time-step size $\Delta t = 0.004\Delta r$. Making the step size smaller was not found to affect the numerical solution significantly.

The numerical scheme (11) is used with r replacing x and

$$\mathbf{U}_j^n = \begin{bmatrix} u_j^n \\ \chi_j^n \end{bmatrix}, \quad \mathbf{F}_j^n = \begin{bmatrix} (u_j^n)^2/2 + \chi_j^n/r \\ u_j^n \chi_j^n \end{bmatrix} \quad \text{and} \quad \mathbf{B}_j = \begin{cases} \begin{bmatrix} 0 \\ 0 \end{bmatrix}, & r > \alpha, \\ \begin{bmatrix} 0 \\ -r_j F/\pi\alpha^2 \end{bmatrix}, & 0 \le r < \alpha. \end{cases}$$

This is subject to the boundary conditions

$$\frac{\partial \zeta}{\partial t} = \frac{\partial u}{\partial t} = 0 \quad \text{at} \quad r = 12,$$

https://doi.org/10.1017/S0334270000011280 Published online by Cambridge University Press

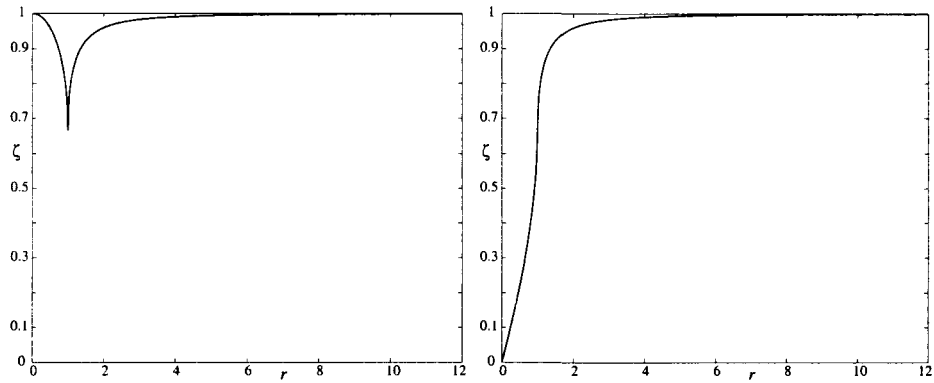

FIGURE 10. The two axi-symmetric free surface elevation profiles for $\alpha = 1$ and critical Froude number $F_{\text{crit}} \approx 3.42$, (a) the stagnation point solution, and (b) the 'drawn-down' solution.

$$u = 0, \quad \frac{\partial \zeta}{\partial t} = -2\zeta \frac{\partial u}{\partial r} - \frac{F}{\pi \alpha^2} \quad \text{at} \quad r = 0. \tag{25}$$

The last boundary condition in the system (25) is obtained from (18) evaluated at $r = 0$. It is discretised using a forward Euler difference for both the time and the space derivative. We note that this boundary condition is less accurate than the numerical scheme being applied to the interior.

First we test the stability of the steady solution for $F = 1$ and $\alpha = 1$ by adding a small perturbation of the form $\zeta_\epsilon = -0.001 r^2 e^{1-r^2}$. The solid line in Figure 11(a) is the full initial condition (with perturbation added), the dotted line corresponds to the steady solution (23) and the difference between them is the perturbation itself, shown here with a dash-dot line. Figures 11(a)–(c) show the time evolution of the perturbation, which can be seen to propagate outwards with decaying amplitude as required. Some instability at the $r = 0$ boundary is observed, due to the boundary condition (25) but this does not greatly impact on the behaviour of the solution. We hence conclude that the solution for $F = 1$ is stable, as expected.

In a similar fashion, the steady solution for $F = 3$ is input as the initial condition for the unsteady problem running with $F = 3.1$. This is equivalent to adding a small perturbation that looks like the steady solution for a tiny Froude number. Again the perturbation is seen to propagate outwards and decrease in amplitude until it hits the far boundary. This is done because we want to use a solution from the steady problem, with Froude number just less than the critical Froude number, as an initial condition for the unsteady problem running with Froude number greater than the critical Froude number $F_{\text{crit}} \approx 3.42013$.

It is found that both the stagnation solution and the second "drawn-down" solution, for the critical Froude number $F_{\text{crit}} \approx 3.42013$, are unstable. Nor were any stable

https://doi.org/10.1017/S0334270000011280 Published online by Cambridge University Press

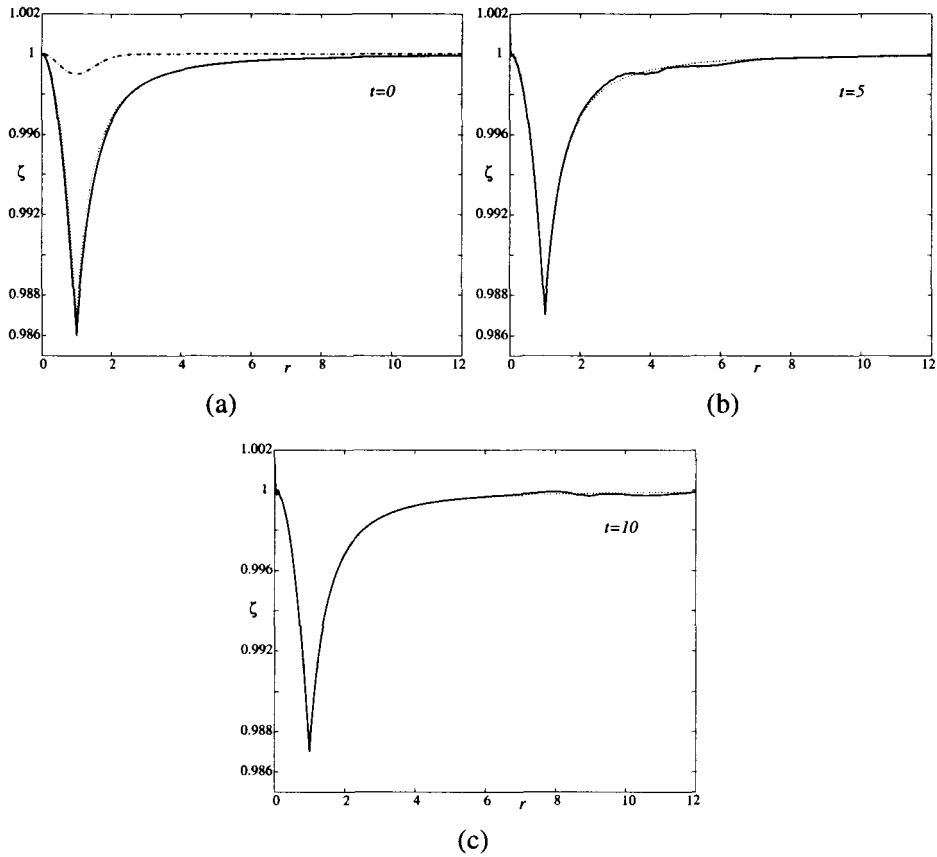

FIGURE 11. The time evolution of a small disturbance to the steady solution, for $\alpha = 1$ and $F = 1$, at times (a) $t = 0$ (dash-dot line is the perturbation) (b) $t = 5$ and (c) $t = 10$, where the solid line is the numerical solution and the dotted line the steady solution.

solutions found for Froude numbers in excess of the critical Froude number. Presumably some different type of flow occurs for F larger than F_{crit} in (24), and it may be the case that the rotating solutions of Forbes and Hocking [2] are encountered in this parameter region.

7. Conclusions

In this paper, the classical shallow water, or hydraulic, theory has been used to analyze the behaviour of two-dimensional and three-dimensional withdrawal flows. In the two-dimensional case, this theory suggests that stagnation-type solutions are only likely in the subcritical region $F < 1$. For supercritical flows, $F > 1$, it appears

https://doi.org/10.1017/S0334270000011280 Published online by Cambridge University Press

that the free surface is drawn right into the drain, similar to the flows computed by Hocking [4], although the numerical calculations for this regime were not conclusive. If this were the case for supercritical flows however, it would suggest that the fully non-linear, supercritical solutions with a free surface stagnation point, computed by Mekias and Vanden-Broeck [9], may in fact be unstable.

For three-dimensional axi-symmetric withdrawal flows, shallow water theory reveals that a limiting flow occurs, at which the surface is again drawn into the sink. However, solutions for larger Froude numbers appear not to exist and it is likely that some radical alteration to the flow takes place. This may explain, in part, the limiting Froude number encountered by Forbes, Hocking and Chandler [3] for flows of this type and perhaps suggests the necessity to allow for the effects of rotation, for Froude numbers beyond the critical, as in Forbes and Hocking [2]. The stability of our subcritical steady solutions to small perturbations has been demonstrated.

8. Acknowledgements

The work of A. J. Koerber has been supported by a Departmental Scholarship from the Department of Mathematics at the University of Queensland and an Australian Postgraduate Award.

References

[1] L. K. Forbes and G. C. Hocking, "Flow caused by a point sink in a fluid having a free surface", *J. Austral. Math. Soc. Ser. B* **32** (1990) 231–249.

[2] L. K. Forbes and G. C. Hocking, "The bath-plug vortex", *J. Fluid Mech.* **284** (1995) 43–62.

[3] L. K. Forbes, G. C. Hocking and G. A. Chandler, "A note on withdrawal through a point sink in fluid of finite depth", *J. Austral. Math. Soc. Ser. B* **37** (1996) 406–416.

[4] G. C. Hocking, "Flow from a vertical slot into a layer of finite depth", *Appl. Math. Modelling* **16** (1992) 300–306.

[5] G. C. Hocking and L. K. Forbes, "Subcritical free-surface flow caused by a line source in a fluid of finite depth", *J. Engin. Math.* **26** (1992) 455–466.

[6] G. N. Ivey and S. Blake, "Axisymmetric withdrawal and inflow in a density-stratified container", *J. Fluid Mech.* **161** (1985) 115–137.

[7] R. J. LeVeque, *Numerical Methods for Conservation Laws* (Birkhäuser Verlag, Basel; Boston; Berlin, 1990).

[8] R. W. MacCormack, "Numerical solution of the interaction of a shock wave with a laminar boundary layer", *Phys. Fluids A* **3** (1971) 2652–2658.

[9] H. Mekias and J.-M. Vanden-Broeck, "Supercritical free-surface flow with a stagnation point due to a submerged source", *Phys. Fluids A* **1** (1989) 1694–1697.

[10] H. Mekias and J.-M. Vanden-Broeck, "Subcritical flow with a stagnation point due to a source beneath a free surface", *Phys. Fluids A* **3** (1991) 2652–2658.

[11] J. J. Stoker, *Water Waves* (Interscience Publishers, Inc., New York, 1957).

[12] E. O. Tuck and J.-M. Vanden-Broeck, "A cusp-like free-surface flow due to a submerged source or sink", *J. Austral. Math. Soc. Ser. B* **25** (1984) 443–450.

[13] Q. Zhou and W.P. Graebel, "Axisymmetric draining of a cylindrical tank with a free surface", *J. Fluid Mech.* **221** (1990) 551–532.